Protein dynamics without energy landscape: principle component analysis with time domain neutron scattering

Wolfgang Doster Technical

University Munich, Physics Department E 13 and FRM 2,

D-85748 Garching, Germany

Abstract

The neutron scattering spectra of dry and hydrated myoglobin are analyzed in the time domain based on a generic dynamic model with two principal components, rotational transitions of side chains, mainly methyl groups and local translational diffusion of non-methyl side chains. The significance of the fits is based on data covering a wide range in time, momentum exchange and temperature. The spectra of three spectrometers with overlapping energy range are Fourier transformed to the time domain from 10^{-13} to 10^{-9} s. In the hydrated case, regular exponential methyl group reorientation is observed on a 10 picosecond time scale. In the dehydrated system this process is slowed down by a factor of two and a further dispersion to even slower correlation times occurs. The local diffusion of non-methyl side chains varies strongly with the water content. It is absent in the dehydrated system. At full hydration, the respective correlation times at 150 ps overlap with those observed for hydration water, suggesting a close coupling. The translation-rotation model applies the established theory of space time correlation functions successfully, which is compatible with the idea of homogeneous quasi-elastic spectra. The temperature dependent elastic intensity extrapolated to zero momentum exchange is derived from the unavoidable effects of multiple scattering, independent of energy landscapes.

Introduction

The first article of this series was concerned with the neutron scattering analysis of fast molecular motions in proteins derived from elastic scattering experiments[1]. In this article we focus directly on inelastic scattering spectra transformed to the time domain. Time domain intermediate scattering functions, de-convoluted from the instrumental resolution function, are easier to interpret than spectra. It is also shown how elastic and energy resolved experiments can be understood on a common basis. Our method is exemplified with data measured with lyophilized and hydrated myoglobin. Similar data sets exist for numerous other proteins[1]. Our goal is to achieve an efficient molecular description in terms of principle components to simplify the complex energy landscape.

The first dynamic neutron scattering experiments at subzero temperatures were performed in 1989 with dry and hydrated myoglobin[2]. Two molecular processes could be distinguished by their temperature dependence using thermally stable D_2O-hydrated powders instead of solutions[3]. In hydrated samples global protein diffusion is arrested, emphasizing the spectral contribution of internal structural fluctuations. Elastic scans versus the temperature revealed two dynamical transitions by the abrupt increase of hydrogen displacements above 150 K and 240 K[2-7]. With an analytical model of the elastic scattering function, the processes were assigned to two-(or three) state transitions of side chains (type I) and water-coupled diffusion on a small scale (type II)[1,2-7]. The type II transition, characterized as a cross-over of relaxation time and instrumental resolution based on the inelastic spectrum, was denoted as a 'dynamical transition' because of its connection with the glass transition of hydration water[2,8]. The low temperature transition at 150-180 K was incorrectly characterized as

a de-trapping of rotational transitions related to the glass transition of hydration water. Today, type II is still assigned to water coupled local diffusion, while type I was shown to reflect mostly rotational transitions of the methyl groups[5-8,33-37]. In the original model the two processes were convoluted sequentially, implying identical scattering sites performing two kinds of motion.

Several attempts to derive analytical models from a structural classification of hydrogen atoms and MD simulations have been published. Up to five components were proposed[9-12]. However, the available data base and the many parameter fits were not sufficient to establish conclusive results. In the "three classes of motion" paper by Hong et al.[9] a wide frequency range combining three spectrometers is presented, but the analysis is based a single averaged Q-value. Dellerue et al.[12] combine inelastic neutron scattering experiments with analytical models and simulations. To represent local diffusion, they use the Dianoux-Volino model of free diffusion inside a sphere. Because of the limited Q-range of the Mibemol spectrometer they could not test the validity of their model. The authors display simulated intermediate scattering functions of main and side chain atoms, depending on the distance from the surface. The first experimental intermediate scattering functions derived from Fourier transformed time of flight spectra of hydrated myoglobin, were published in ref. (2). A much improved Q-dependent intermediate scattering function of myoglobin hydration water, indicating anomalous diffusion, was published in 1996[13]. But a time domain analysis is rarely performed. Often time domain simulations combined with elastic scattering experiment[9,20].

Today, after 30 years of effort combining neutron scattering experiments with computer simulations, there is still no accepted model of molecular motions in proteins[6,14-20]. Parallel to the molecular approach, phenomenological models prevail:

Proteins are pictured as partially disordered systems, which are controlled by complex energy landscapes[14,15], dynamical heterogeneity distributions[16,17] and the softening of overall protein force constants[18-20]. In a series of PNAS publications, Frauenfelder et al.[14,15] postulate that neutron scattering spectra of complex systems have to be heterogeneous, which would invalidate the well-established theory of Van Hove space-time correlation functions[5,21-23]. Moreover the well-known effect of a temperature dependent elastic intensity at zero momentum exchange is interpreted to prove of the heterogeneous spectral model of energy landscapes. By time domain analysis and multiple scattering calculations, we test some of the main assumptions of this model.

The phenomenological approach ignores the potential of neutron scattering to provide molecular insight complementary to simulations. Neutron scattering emphasizes the hydrogens, which constitute nearly half of the atoms in proteins. They mediate H-bridges in helices and take part in other nonbonding interactions of electrostatic and van der Waals forces. Polar bonds play a critical role in enzyme catalysis, substrate binding and proton transfer reactions. Main chain and side chain hydrogens contribute to the stability of the protein secondary structure and mediate structural fluctuations. Neutron diffraction yields precise hydrogen positions and fluctuation amplitudes in excess to x-ray crystallography, since the hydrogen neutron cross section is comparable to the carbon[11,24]. A particularly useful property of the proton is its large incoherent cross section, about ten times larger than those of other atoms. As a result, 85 % of the scattering amplitude of proteins reflects hydrogen atoms[24]. Incoherent dynamic neutron scattering is a unique tool to record time resolved the average displacements of single hydrogen atoms on a sub- nanosecond time scale[5,13]: The scattering contribution of hydration water in D_2O-hydrated powders can be kept as

low as 4 % [24]. Energy resolved spectra, Fourier-transformed to the time domain, yield a hydrogen weighted density correlation function of structural fluctuations. We employ high quality spectra combining three neutron spectrometers, which are transformed to the time domain covering a wide Q-range. From this new data base we derive a model of minimal complexity, comprising the original two principle types of molecular motions[2,5] .

The basic physical quantity to be determined in the case of proteins is the density self-correlation function $G_s(\vec{r}, t)$ characterizing the distribution of single particle displacements $\vec{r}$ within time t. For isotropic powder samples only the magnitude of $\vec{r}$ matters. In scattering experiments one measures the intermediate scattering function in momentum-space, which is the Fourier transform of the density correlation function[21-23]:

$$\Phi_s(Q,t) = < \int d^3\vec{r} \cdot e^{-i\vec{Q}\cdot\vec{r}} G_s(\vec{r},t) >_{powder} \qquad (1)$$

The resulting powder averaged intermediate scattering function $\Phi_s(Q, t)$ of N hydrogen atoms is then given by [5,23]:

$$\Phi_s(Q,t) = \frac{1}{N}\sum_i \Phi_i(Q,t)) = \frac{1}{N}\sum_i \exp\left[-Q^2\left\langle \Delta x_i^2(t)\right\rangle/2 + Q^4 .....\right] \qquad (2)$$

Q is the magnitude of the scattering vector, $Q = 4\pi/\lambda \sin(\theta/2)$, λ denotes the incoming neutron wavelength and θ is the scattering angle relative to the incident direction. In equ.(2) we indicate the moment expansion of the powder averaged hydrogen displacement distribution $G_s(r, t)$. The second moment, $<\Delta x_i^2(t)>$, defines the mean square displacement (MSD) of a specific site 'i' at time t. Expanding $\Phi_s(Q\rightarrow 0, t)$ in the "Gaussian" approximation yields the site averaged MSD: $<\Delta x^2>_t = \Sigma<\Delta x_i^2>/N$.

Most bio-neutron scattering studies up to date deal with elastic scattering experiments[1]. Temperature dependent MSD scans were measured for numerous proteins under different environmental conditions. Fig. 1 summarizes some essential results for myoglobin[5]: Vibrational displacements are characterized by a linear MSD temperature dependence. A prominent example is provided by myoglobin embedded in a D-exchanged hydrogenated sucrose glass, suggesting that vitrified proteins do not move[18,19]. By contrast, with myoglobin embedded in a fully deuterated glass, D-glucose, a strong nonlinear enhancement of $<\Delta x^2>(T)$ at 150 K appears[5]. Strikingly, dehydrated myoglobin exhibits about the same MSD temperature dependence as myoglobin vitrified in a per-deuterated glass[5].

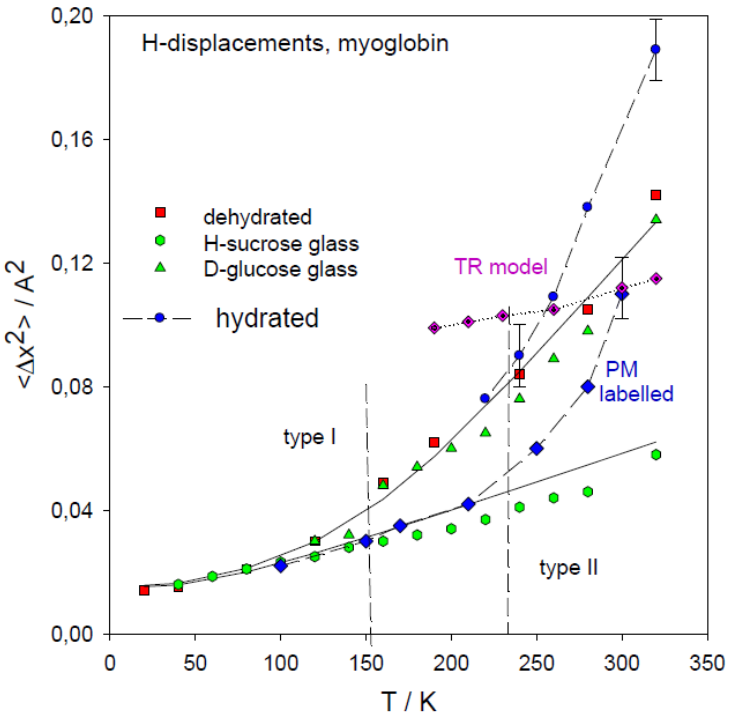

Fig. 1: MSD (IN13, τ_{res} = 140 ps) of myoglobin in various environments[1,5]: dehydrated (red squares), hydrated (blue circles), green triangles: per-deuterated glucose glass, green circles: D-H-sucrose glass[18,19], blue diamonds: H-labelled per-deuterated PM fragments[18], violet diamonds: δ^2 of TR model, thick line: predicted

methyl group displacements[5], thin line: calculated f vibrational displacemen[25,26]. The onset temperatures at 150 K (I) and 240 K (II) are indicated.

The type I transition at 150 K is thus attributed to the onset of protein internal motions, which are not sensitive to changes of the protein environment. By contrast, with D_2O-hydrated myoglobin, two transition temperatures at 150 K (type I) and 240 K (type II) are recorded, suggesting two well separated molecular processes. Since the second transition (type II) does not occur without water, these motions were assigned to protein displacements related to a wet protein surface[2,5]. Since the scattering fraction of hydration water (D_2O) amounts to less than 5 %, type II motions characterize the indirect effect of hydration on structural fluctuations. Experiments performed with "wet" per-deuterated purple membrane fragments yield similar, noisier MSD scans with two transitions at the same temperatures 150 and 240 K. By contrast, if the per-deuterated purple membrane fragments are specifically labelled with protonated, but methyl-free residues, the type I transition is missing, although type II at 240 K is still occurs[18,19]. This indicates, that type I displacements reflect mostly methyl side chains[5,6]. Then Type II by contrast must involve prominently polar residues near the surface. An indirect effect of hydration on the mobility of nonpolar, non-methyl side chains by swelling effects cannot be excluded. With too much solvent, type I is missing and melting of D_2O interferes with type II [27]. With cryo-solutions protein diffusion has to be accounted for[28,29]. Only a single dynamic transition at ~200 K is observed with Mössbauer spectroscopy, recording the motions of the heme iron. It was assigned recently to type II, depending strongly on the solvent viscosity[1,30].

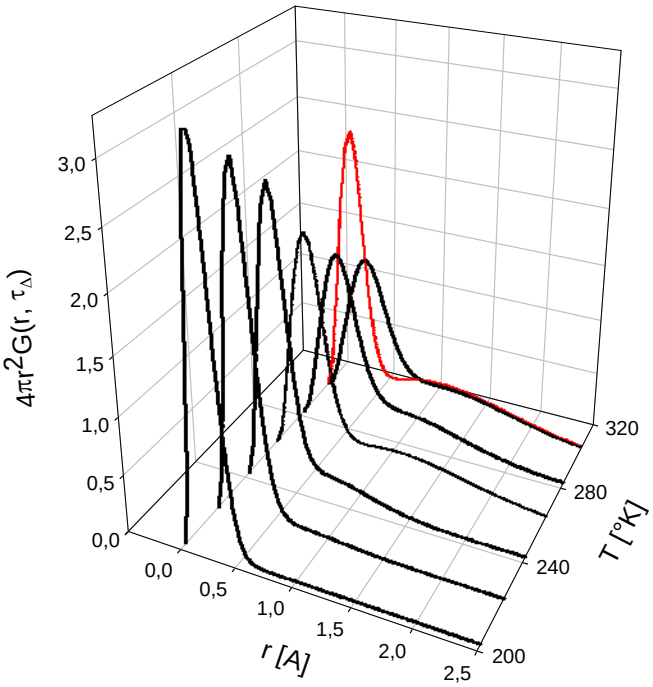

Fig. 2: Displacement distribution functions of dry (red, 300 K) and hydrated myoglobin versus displacement r and the temperature.

The second moment reflects only the low Q part of the elastic scattering function. By inverting equation (1), the powder averaged displacement distribution $G_s(r, t)$ could be reconstructed from $\Phi_s(Q, t)$, in principle. A valuable method uses elastic scans, which approximate the $\Phi(Q, t = \tau_{res})$ at the fixed resolution time of the spectrometer: Fitting the experimental elastic scattering functions using a series of Gaussians as with the dynamical heterogeneity approach[16,17], a powder averaged displacement distribution $4\pi r^2 G(r, \tau_{res})$ could be constructed for myoglobin[5]. Fig. 2 shows the essentially bimodal distribution function and its evolution with the temperature. Below 200 K only one maximum is observed reflecting vibrational motions. Above 200 K, two peaks at r ≅ 0,5 Å and 1,5 Å appear. The second maximum (type I) occurs in hydrated, but also in dehydrated (red) and glassy protein environments. It accounts for the low temperature enhancement of average hydrogen displacements above 150 K. The maximum, reflecting small scale displacements, vibration and local diffusion, appears only with hydrated proteins as the red curve shows. It is connected with the onset of un-harmonic displacements above 240 K. This suggests the involvement of polar side chains near the protein surface of type II.

Methods

Previous dynamic neutron scattering experiments performed with the spectrometers IN6, IN10 and IN13 at the ILL in Grenoble were reanalyzed. The frequency domain spectra are transformed to the time domain[13]. Taken together this new analysis covers a large Q-range up to 5 $Å^{-1}$, combined with a time window ranging from 0,1 to 1000 picoseconds. The recorded dynamical structure factor, $S(\theta, \hbar\omega)$, versus scattering angle θ and energy exchange $\hbar\omega$, is first recalculated at a constant Q format, $S(Q, \hbar\omega)$, which is then symmetrized by the detailed-balance factor. The time domain correlation function $\Phi_s(Q, t)$ is determined numerically by turning the Fourier integral of $S(Q, \omega)$ into a sum of discrete points using the experimental spectrum $S(Q, \omega_j)$:

$$\Phi_s(Q,t) = \hbar \int d\omega e^{i\omega \cdot t} S(Q,\omega) \cong \hbar \cdot \Delta\omega \cdot \sum_j e^{i\omega_j \cdot t} S(Q,\omega_j) \qquad (3)$$

To avoid aliasing effects the smooth spectra $S(Q, \omega_j)$ are interpolated with a maximum number of n data points according to $t_n = n \cdot \frac{\pi}{\omega_{max}}$ (FFT), where ω_{max} is the cut-off frequency of the spectrum. As a consistency check the transformed result is back-transformed to the frequency domain. To de-convolute the data from the resolution function, a time domain low temperature spectrum of Mb-D_2O at 100 K was determined. The elastic intensity was collected using a fixed energy window method (τ_{res} = 140 ps) and the back-scattering spectrometer IN13[21]. With 350 mg of D_2O hydrated horse myoglobin (h = 0,35-0,38 g/g), the neutron transmission was close to a tolerable 90 %. Raw data were corrected for detector response and cell scattering.

Results

a) Definition of the translation-rotation model (TR)

Motivated by the results of fig. 1 and 2, we propose a bimodal distribution of sites associated with two kinds of motions: (I) internal rotational transitions and local translational diffusive displacements (II). Thus a bimodal correlation function of principle components is assumed:

$$\Phi_s(Q,t) = \sigma_I \cdot \Phi_I(Q,t) + (1-\sigma_I) \cdot \Phi_{II}(Q,t) \quad (4)$$

σ_I denotes the fractional cross section of the type I sites.

Equ. (4) must be complemented by a term accounting for global protein diffusion, if the degree of hydration exceeds 0,4 g/g or in solution.

According to the neutron structure of myoglobin[11] 25 -28 % of the total number of hydrogens are organized in methyl groups, thus $\sigma_I = \sigma_m \cong 0{,}25$ -0,28.

More specifically, type I motions are defined by a three site jump model of methyl groups reorienting by 120° jumps about their three-fold symmetry axis[21]:

$$\Phi_{rot}(Q,t) = \frac{1}{3}\{1 + 2\,j_0(Q) + 2 \cdot (1 - j_0(Q)) \cdot \exp(-t/\tau_{rot})\} \quad (5)$$

$$j_0(Q) = \sin(Q\sqrt{3} \cdot r)/(Q\sqrt{3} \cdot r)$$

is the zero order Bessel function, where r = 1,03 Å is the length of the C-H bond.

Exponential relaxation or a single barrier height is assumed for simplicity. Note that $\tau_{rot} = \tau_{Met}/3$ and that the $EISF_{met}(Q) = \Phi(Q, t >> \tau_{rot})$ is not Gaussian.

By contrast, type II processes involve small local displacements of residues confined by a quasi- harmonic potential, which is approximate by an over-damped Brownian oscillator[31,32]:

$$\Phi_{trans}(Q,t) = \exp\{-Q^2\delta^2 \cdot (1 - \exp(-t/\tau_{trans}))\} \quad (6)$$

$\delta^2 = \langle \Delta x^2 \rangle_{trans}$ denotes the translational mean square displacement, which is apart from the time constants, the main free parameter of the model. At long times, $\Phi_{trans}(Q,\ t >> \tau_{trans})$ turns into a Gaussian elastic scattering function:

$$\Phi_{trans}(Q, t >> \tau_{trans}) = \exp(-Q^2 \cdot \delta^2) \qquad (7)$$

The TR-model with two principal components is defined by the equations 4 – 6.

b) Time domain analysis

Fig. 3 displays the combination of the transformed intermediate scattering functions of dry and D_2O hydrated myoglobin at 300 K. The initial decay at 0,1 picoseconds reflects the vibrational dephasing of the Boson peak, which differs for dry and hydrated myoglobin[4]. We focus on the over-damped regime above 1ps, where the correlation functions have been normalized.

In the hydrated case, the decay of the correlation function covers at least three decades, which is difficult to interpret without assistance of a theoretical model.

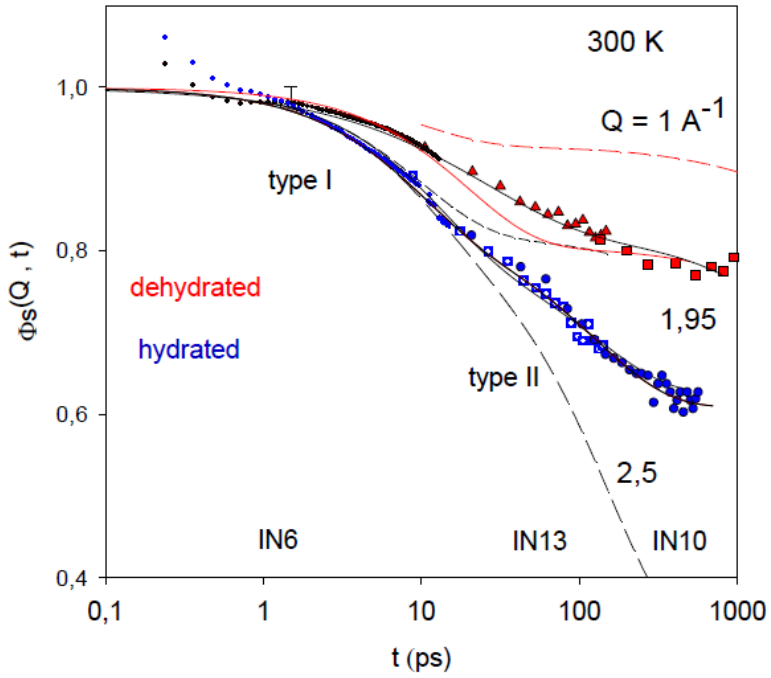

Fig. 3: Density correlation function of dry and hydrated myoglobin at 300 K and Q = 1,95 Å^{-1}, combining the spectral information of three instruments as indicated, h = 0,35 g/g (blue), h < 0,05 g/g (red). Full line: fits to equs.4 - 6 adjusting the time constants, τ_{rot} = 9 (±1) ps, τ_{trans}= 145 (±10) ps and δ^2= 0,11 (±0,015) Å^2. Dashed

line, type I only, red triangles and squares: dehydrated myoglobin, red line: type I fit, τ_{rot} = 18 (±2) ps, σ_m =0,25, black line: fit to a stretched exponential, exponent: 0,7

The full line shows the prediction of the TR model at Q = 1,95 $Å^{-1}$ to be accurate. Alternative predictions at Q = 1 and 2,5 $Å^{-1}$ deviate strongly, illustrating the sensitivity of the model. The methyl group relaxation is well represented by an exponential decay (short dash), leading to a Q-dependent long-time plateau at 0,8. The Brownian oscillator correlation function is non-exponential. Its long time value is given by equ. 7. We derive two well separated components with time constants at τ_{rot} = 9 (±1) ps and τ_{trans} = 145 (±15) ps. This result confirms the analysis of figs. 1 and 2 displaying two well separated onset temperatures and displacement distribution maxima. The barrier to methyl group rotation in proteins amounts to12 kJ/mol[5,33-37]. With a pre-factor of 10^{-13}s one obtains 11 ps, compatible with the interpretation of type I.

The second time constant τ_{trans} overlaps with experimental correlation times of protein hydration water (fig. 6), supporting a polar origin of type II. By fitting IN10 spectra of myoglobin-D_2O in the frequency domain, we derive a linewidth corresponding to τ_{trans} = 150 (±10) ps. A mean square displacement parameter of δ^2 = 0,11 (± 0,015) $Å^2$ is deduced. The alternative fits show the variation of σ_m = 0,24 to 0,28, accounting for further methyl-like transitions.

In the dehydrated case, the second decay of type II is significantly reduced as expected. Most important, drying slows down methyl group reorientation by more than a factor of two. The fit to equ. 5 yields τ_{rot}(dry) = 18 (± 2) ps. We have checked this result by a spectral analysis of dry and hydrated myoglobin using IN6 and IN10. We obtain τ_{rot}(hydrated) ≅ 8,5 ps and 19 (± 2) ps for the dehydrated case, similar to the time domain results. Interestingly, the TR model fits disagree with the data at intermediate times ≅ 50 ps. The fit to a stretched exponential with a stretching exponent of 0,7 and τ_{rot}≅ 25 ps can account for the full time range. Dehydration thus induces a dispersion of methyl side chains with increased barrier in a more compact rigid environment. However, the important long time plateau value of ≅0,8 is identical with the hydrated case, supporting the assignment to methyl groups only.

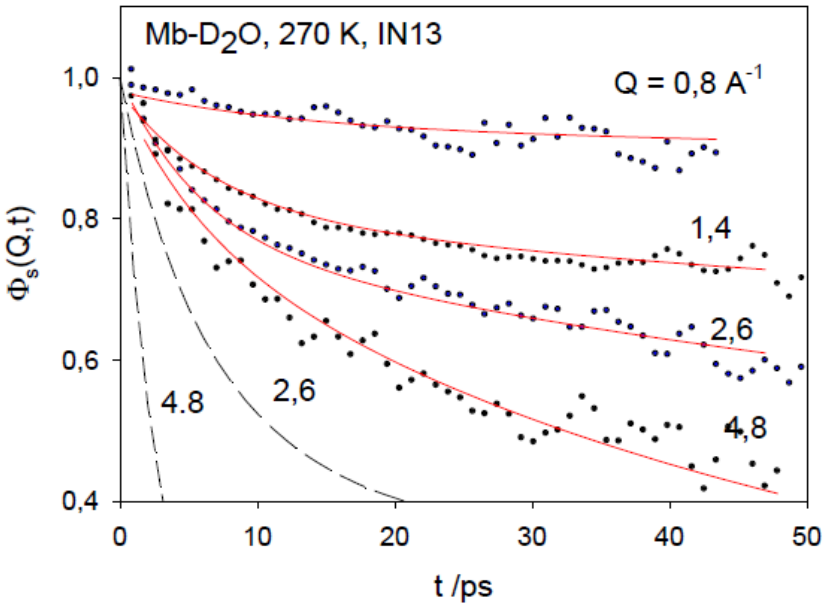

Fig. 4: Time domain density correlation function $\Phi_s(Q, t)$ of myoglobin-D_2O (0,35 g/g) (IN13) at various Q values. The red lines are the predictions of the TR model with $\delta^2 = 0{,}11(\pm 0{,}02)A^2$, $\tau_{rot} \cong 11$ (±2)ps and $\tau_{trans} \cong 155$ (±20) ps at 270 K. The dashed lines are the predictions of the Brownian oscillator of equ.6.

Fig. 4 shows the intermediate scattering function of hydrated myoglobin covering an extended Q-range up to 4,8 $Å^{-1}$ at a slightly reduced time window. The fits to the TR model are conclusive, if we use the correlation times determined above as input (fig. 3). The MSD is adjusted, yielding, $\delta^2 = 0{,}09$ (±0,02) $Å^2$. The Brownian oscillator (equ. 6) would predict a much stronger Q-dependence. The quality of the fit, indicates, that the TR model reproduces the spatial distribution of displacements rather well.

c) Temperature dependent dynamics from elastic scans

The elastic scattering profiles, measured with hydrated myoglobin are shown in fig. 5a, normalized at the lowest temperature of 10 K. To unravel the dynamic aspects of elastic scattering in a transparent manner, we have introduced the method of "elastic resolution spectroscopy"[1,7], where the resolution function is varied. In the simplest case of a δ-correlated resolution function[1], the normalized elastic intensity versus Q accurately reproduces the time correlation function at fixed resolution time:

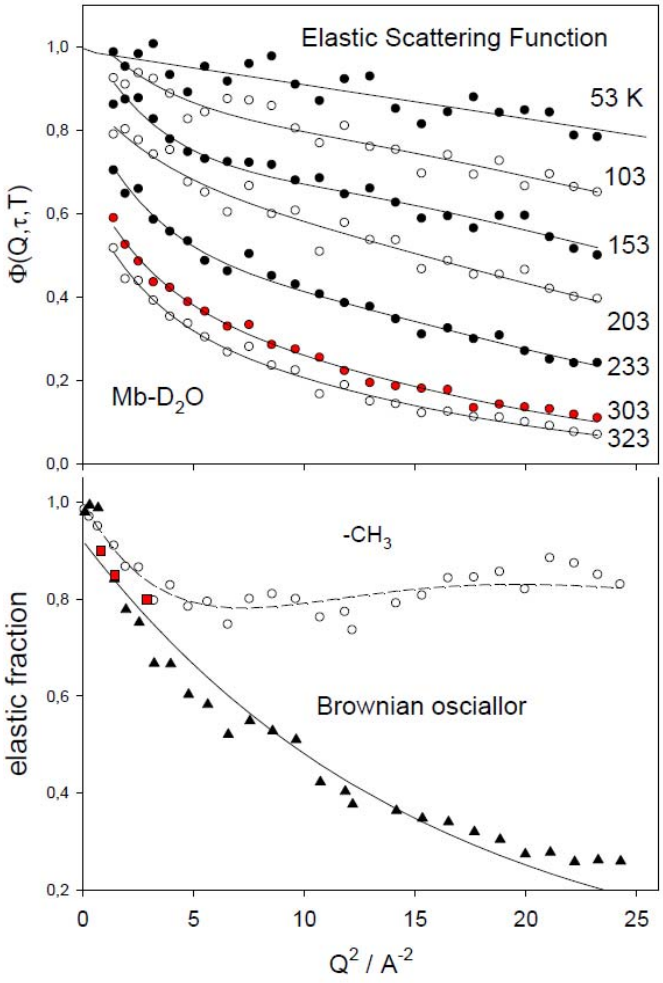

Fig.5 a): Elastic scattering profiles of hydrated myoglobin (0,35 g/g) normalized at 10 K, back-scattering spectrometer IN13 at τ_{res}*= 140 ps and TR-fits by adjusting* $\tau_{rot}(T)$ *and* $\tau_{trans}(T)$ *with* δ^2*= 0,1 Å*^{2} *kept fixed (full line).*

b) *Decomposition of the elastic scattering function of hydrated myoglobin at* 270 K *according to the TR-model, the full lines are predictions of equs.5 and 6. Red squares: lysozyme, HFBS*[6,34]

$$S_{el}^{N}(Q) \cong \Phi_s(Q, \tau_{res}) \qquad (8)$$

Thus by fitting elastic scans versus momentum exchange at fixed time τ_{res} by adjusting $\tau_{rot}(T)$ and $\tau_{trans}(T)$ in equs. 4 - 6, yields the requested dynamic information. At the next level of approximation the time functions in equ. 5 and 6 are replaced by a convolute with the exact resolution function of the spectrometer[1]. For the methyl

group this analysis has been performed with dehydrated myoglobin, resulting in a prediction of the MSD(T) shown in fig. 1[5]. In the present context this procedure works rather well already at the level of equ. 8. The most striking result is the absence of dynamical transitions: The fitted MSD parameter, $\delta^2 \cong 0{,}1$ Å^2 is almost independent of the temperature as demonstrated in fig. 1.

As an example, fig. 5 b) shows a decomposition of the elastic scan at 270 K into a Gaussian (Brownian oscillator) and the methyl incoherent structure factor based on the TR model. Note the limited Q-range of the HFBS spectrometer, which is often cited in the context of methyl rotation[34]. Equally important, the resulting correlation times $\tau_{rot}(T)$, displayed in fig. 6, compare well with those determined independently by a spectral analysis of dehydrated myoglobin and the methyl side chain of alanine dipeptide[1]. The methyl barrier in the hydrated case is 11 (± 1) kJ/mol, the pre-exponential amounts to 1,6 10^{13}s^{-1}.

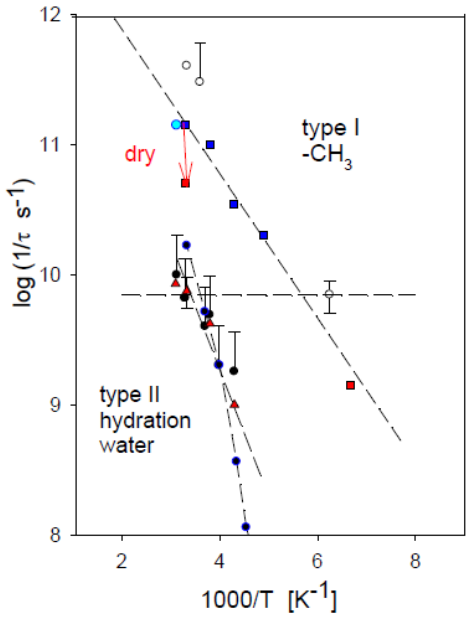

Fig. 6: Arrhenius plot of the fitted correlation times, τ_{rot}: blue squares: TR model fit, open circles: alanine dipeptide[1], blue circle: spectral analysis of hydrated myoglobin, IN10, red squares: fit of IN6 spectrum of dry myoglobin, τ_{trans}: red triangles: TR model fit, blue and black circles: τ_{hyd} , hydration water[1,8], dashed line: τ_{res} = 140 ps (Instrument IN13)

Also, the translational correlation times, $\tau_{trans}(T)$, superimpose within experimental error with those derived for protein hydration water by neutron spectroscopy[1,8]. The type II barrier is 17 (±1) kJ/mol with a pre-exponential of 7,5 10^{12} s^{-1}.

d) Multiple scattering

The analysis presented above assumes that each neutron on its passage through the sample is scattered only once. In real experiments at a usual transmission near 90% about 17 % of the neutrons are scattered twice[21,25,26]. Although multiple scattering is significant, it is rarely taken into account, because corrections are involved. Elastic-elastic second scattering events yield the dominant contribution due to the large dynamical structure factor of proteins at $\omega = 0$. The second scattering is approximately angle independent, which leads to an extra intensity at $Q = 0$. Since the elastic intensity decreases with temperature rise, multiple scattering also

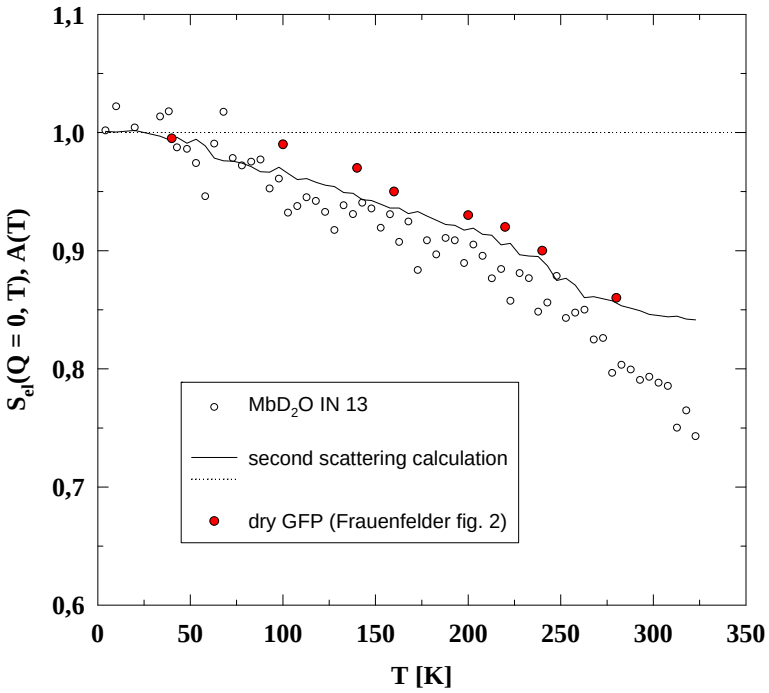

Fig. 7: Multiple scattering derived from extrapolation of the elastic intensity (fig. 5a) to Q = 0 of hydrated myoglobin and (red points) of dehydrated GFP[14], full line: second scattering calculation assuming only elastic-elastic scattering from an infinite flat cell.

decreases. As a result, one always observes with elastic scans an extra intensity at Q = 0, which is decreasing with the temperature: $S_{el}(Q = 0, T)$. Therefore elastic scattering profiles, not fig. 5a, are often normalized at each temperature and Q = 0. Several examples are given in ref.(14), which are incompatible with single scattering theory, violating particle conservation. This discrepancy has recently been used as a main argument against conventional scattering theory. In fig. 7 we display the elastic intensities derived from data presented partially in fig. 5a), which were extrapolated to Q = 0. It shows the effect of a temperature dependent zero Q elastic intensity. Also shown are our calculations of the second order scattering for an infinite plane slap sample according to the method of Sears [21]. The calculated elastic-elastic second scattering curve reproduces the experiment rather well except at high temperatures, where quasi-elastic scattering dominates. Also shown are the reconstructed elastic intensities at zero Q of the green fluorescent protein [14,15]. Given the uncertainties of their extrapolation procedure and the unknown transmission, the agreement is striking. Multiple scattering is thus a valid explanation for the GFP results. Before energy landscapes come into play, one has to correct first for the unavoidable multiple scattering effects and, by the way, the finite instrumental resolution, as shown above.

Discussion

The TR model with only two principal components can reproduce the experimental data of hydrated myoglobin remarkably well, supporting the idea of an efficient description of protein dynamics. This success is partially the result of two components, which are well separated in the time and space. This leaves little room for alternative fits. No evidence of further components due to nonpolar side chains and the main chain was found at this level.

It took more than 10 years until the important role of the methyl group in neutron scattering spectra of proteins was recognized. In 2001, the fast component of the intermediate scattering function of hydrated myoglobin at room temperature was assigned to methyl rotation[7]. Since the time domain data, comparable those of fig. 3, were derived from elastic scattering spectra, the relevance of the resolution function in the dynamical transitions was established[1,5,7]. An extensive analysis of displacement distributions in proteins was published in 2005[5], where type I was definitely identified with methyl group rotation. Roh et al.[34], published slightly later an assignment of an

non-harmonic MSD onset at 100 K to methyl rotation. Their onset temperature is rather low, compared to 150 K (140 K, IN10) of the type I transition[35]. Commercial preparations sometimes contain acetate and thus fast rotating acetyl groups, which cannot be easily removed.

The first temperature and hydration dependent simulation of methyl groups in proteins was published in 2002 by Curtis et al.[33], suggesting, that in the dry case rotation is almost arrested. In the experiment, such transitions are observed, although the transition rates are slowed down significantly. Furthermore, the dispersion of correlation times, deviating from exponential decay suggests a barrier distribution, which is not present in the hydrated case. Dehydration leads to a more compact and rigid structure, which can differ between sites. A distribution of methyl barriers in lyophilized proteins with different structure was reported, applying a similar elastic analysis as in ref.(5)[36]. Methyl groups in proteins have also been observed by other methods like NMR[37]. But the type II water-coupled motions were first discovered by neutron scattering[2]. Hydration water induces swelling, decreasing the local viscosity and, most important, dynamical heterogeneity. The relevance of type II motions suggests a viscoelastic coupling of density fluctuations of hydration water and polar protein residues. This effect is better characterized as plasticization than by "slaving". Simulations suggest a mutual relaxation of the protein-solvent hydrogen bond network via solvent translational motion[33]. The postulate of heterogeneous quasi-elastic spectra[14,15] is not confirmed by our space-time analysis. We derive time constants of molecular processes, which are well established in the literature by other methods. If the spectra would be inhomogeneous, the TR model would fail. Our results thus provide no case against scattering theory[38]. The temperature dependent elastic intensity at zero momentum exchange has to be assigned mostly to multiple scattering and does not support the landscape approach. We also exclude the idea of a change in the protein force constants at the dynamical transition temperature[18]. In the TR model both transitions are removed by accounting for structural relaxation and a finite energy window $\hbar / \tau_{res}$ (fig. 1). This model unifies elastic scattering, as described in the first article,[1] and time domain neutron scattering using a principle component analysis. With an improved data base, it may become possible to identify further dynamic components. **Acknowledgements:** I appreciate the assistance of the instrument scientists Winfried Petry and Bernhard Frick.

References

1. Doster, W., Nakagawa, H., Appavou, M.S. Scaling analysis of bio-molecular dynamics derived from elastic neutron scattering experiments. J. Chem. Phys. **139,** 45105 -16 (2013)
2. Doster, W., Cusack, S., Petry, W. Dynamical transition of myoglobin revealed by inelastic neutron scattering. Nature **337**, 754-756 (1989)
3. Doster, A., Bachleitner, A., Dunau, R., Hiebl, M., Lüscher, E. Thermal properties of water in myoglobin crystals and solutions at subzero temperatures, Biophy. J. **50**, 213-219 (1986)
4. Diehl, M., Doster, W., Petry, W., Schober, H. Water coupled low frequency modes of myoglobin and lysozyme observed by inelastic neutron scattering, Biophys. J. **73**, 2726-2732 (1997)
5. Doster, W., Settles, M., Protein-water displacement distributions. Biochim.Biophys. Act.**1749**,173-186 (2005)
6. Doster, W., Concepts and misconceptions of the protein dynamical transition, Eur. Biophys. J. **37**, 591-602 (2008)
7. Doster, W., Diehl, M., Petry, W., Ferrand, M., Elastic resolution spectroscopy: a method to study molecular motions in small biological samples. Physica B **301**, 65-68 (2001)
8. Doster, W., Busch, S., Gaspar, A., Appavou, M.S., Wuttke, J. . Scheer, J. Dynamical transition of protein hydration water, Phys. Rev. Lett. **104**, 098101-4 (2010)
9. Hong, L., Smolin, N., Lindner, B., Sokolov, A. P., Smith, J., C., Three classes of motion in the dynamic neutron scattering susceptibility of a globular protein. Phys. Rev. Lett. **107**, 148102 (2011)
10. Fitter, J., Lechner, R. E., Büldt, G., Dencher, N.,A.. Internal molecular motions of bacteriorhodopsin: hydration induced flexibility studied by quasi-elastic incoherent neutron scattering using oriented purple membranes, PNAS **93**, 7600-7605 (1996)
11. Engler, N., Ostermann, A., Niimura, N, Parak, F. Hydrogen atoms in proteins: positions and dynamics, Proc. Natl. Acad. Sci. USA**. 100**,10243-10248 (2003)
12. Dellerue, S., Petrescu, A.-J., Smith, J., C., Bellissent-Funel, M., C., Radially softening diffusive motions in a globular protein. Biophys. J. **81**, 1666-1676 (2001)

13. Settles, M., Doster, W., Anomalous diffusion of adsorbed water, a neutron scattering study of hydrated myoglobin, Faraday Disc. **103**, 269-280 (1996)
14. Frauenfelder, H., Young, R. D., Fenimore, P.W. The role of momentum transfer during incoherent neutron scattering is explained by the energy landscape model. Proc. Natl. Acad. Sci. USA **114**, 5130-5135 (2017)
15. Frauenfelder, H., Fenimore, P.W., Young, R.D. A wave-mechanical model of incoherent quasi-elastic scattering in complex systems. PNAS USA **111**, 12764-12768 (2014).
16. Peters, J., Kneller, G.,R., Motional heterogeneity in human acetylcholesterinesterase revealed by a non-Gaussian model for elastic incoherent neutron scattering. J. Chem. Phys.**139**, 165102 1-5 (2013)
17. Becker, T, Smith, J. C. Energy resolution and dynamical heterogeneity effects on elastic neutron scattering. Phys. Rev. E. **67**, 21904-8 (2003)
18. Zaccai, J., How soft is a protein, a protein dynamics force constant measured by neutron scattering. Science **288**, 1604-1607 (2000)
19. Gabel, F., Bicout, D., Lehnert, U., Tehei, M., Weik, M., Zaccai, G. Protein dynamics studied by neutron scattering, Qu. Rev. Bioph. **35**, 327-367 (2002)
20. Hong, L.,Glass, D., C., Nickels, J., D., Perticaroli, S., Zheng, Y., Madhusudan, T., O'Neill, H., Zang, jQ., Sokolov, A., P., Smith, J., C., Elastic and conformational softness of a globular protein. Phys. Rev. Lett. **110**, 028104-1 ,-5 ((2013)
21. Bee, M., Quasielastic Neutron Scattering. p. 17, 107-147, 195 Adam Hilger, Bristol, Philadelphia (1988)
22. Squires, G. L. Introduction to the theory of thermal neutron scattering, Dover Books in Physics p. 101 (1978)
23. Lovesy, S., W., Dynamics of solids and liquids by neutron scattering, p. 1-10, Springer Verlag Heidelberg (1977)
24. Gaspar, A.M., Busch, S., Appavou, M., S., Häussler, W., Georgii, R., Su, Y., Doster, W. Using polarization analysis to separate coherent and incoherent scattering from protein samples, Biochim. Biophys. Act. **1804**, 76-82 (2010)
25. Cusack, S., Doster, W. Temperature dependence of the low frequency dynamics of myoglobin. Biophys. J. **58**, 243-251 (1990)
26. Settles, M., Doster, W. Iterative calculations of the vibrational density of states from incoherent neutron scattering data with the account of double scattering. Biological Macromolecular Dynamics, 3-8, Adenine Press (1997)

27. Ferrand, M., Dianoux, A. J., Petry, W., Zaccai, G. Thermal motions and function of bacteriorhodopsin in purple membranes: Effects of temperature and hydration studied by neutron scattering. Proc. Natl. Acad. Sci. USA, **90**, 9668-9672 (1993)
28. Daniel, R., Finney, J., Reat, V., Dunn, R., Ferrand, M., M., Smith, J. Enzyme dynamics and activity: time scale dependence of dynamical transitions in glutamate dehydrogenase solution. Biophys. J. 77**,** 2184-2190 (1999)
29. Gaspar, A., M., Appavou, M., S., Busch, S., Unruh, T., Doster, W. Dynamics of well folded and disordered proteins in solution: a time of flight neutron scattering study. Eur. Biophys. J. **37**, 573-582 (2008)
30. Lichtenegger, H., Doster, W., Kleinert, T., Birk, A., Sepiol, B., Vogl, G., Heme solvent coupling, a Mößbauer study of myoglobin in sucrose. Bioph. J. **76**, 414-422 (1999)
31. Doster, W. Brownian oscillator analysis of molecular motions in biomolecules in 'Neutron Scattering in Biology, techniques and applications' Eds. Fitter, J., Gutberlet, T., Katsaras, J., Springer, biological and medical physics, biomedical engineering , chapter 20, 461-482 ((2006)
32. Risken, H. The Fokker Planck equation; methods of solution and applications, Springer , Berlin (1984)
33. Curtis, J.E, Tarek, M., Tobias, D.J. Methyl group dynamics as a probe of the protein dynamical transition, JACS **126**, 15929 (2004)
34. Roh, J.,H., Novikov, V., Gregory, R., Curtis, J., Chowdhuri, Z., Sokolov, A. Onsets of non-harmonicity in protein dynamics , Phys. Rev. Lett. **95**, 38101-1,4 (2005)
35. Chiro, G., Caronna, Ch., Natali, F., Cupane, A. Direct evidence of the amino acid side chain and backbone contributions to protein anharmonicity. J. Am. Chem. Soc. **132**, 1372-74 (2010)
36. Telling, M., T., F., Clifton, L., Combet, J., Frick, B., Howells, S., Garcia Sakai, V., Lyophilised protein dynamics: more than just methyls? Soft Matter **8**, 9529-9532 (2012)
37. Lee, A., L., Wand, A., J., Microscopic origins of heat capacity and the glass transition in proteins. Nature **411**, 501-504 (2001)
38. Wuttke, J. No case against scattering theory, Proc. Natl. Acad. Sci. USA **114**, E8318/19 (2017)

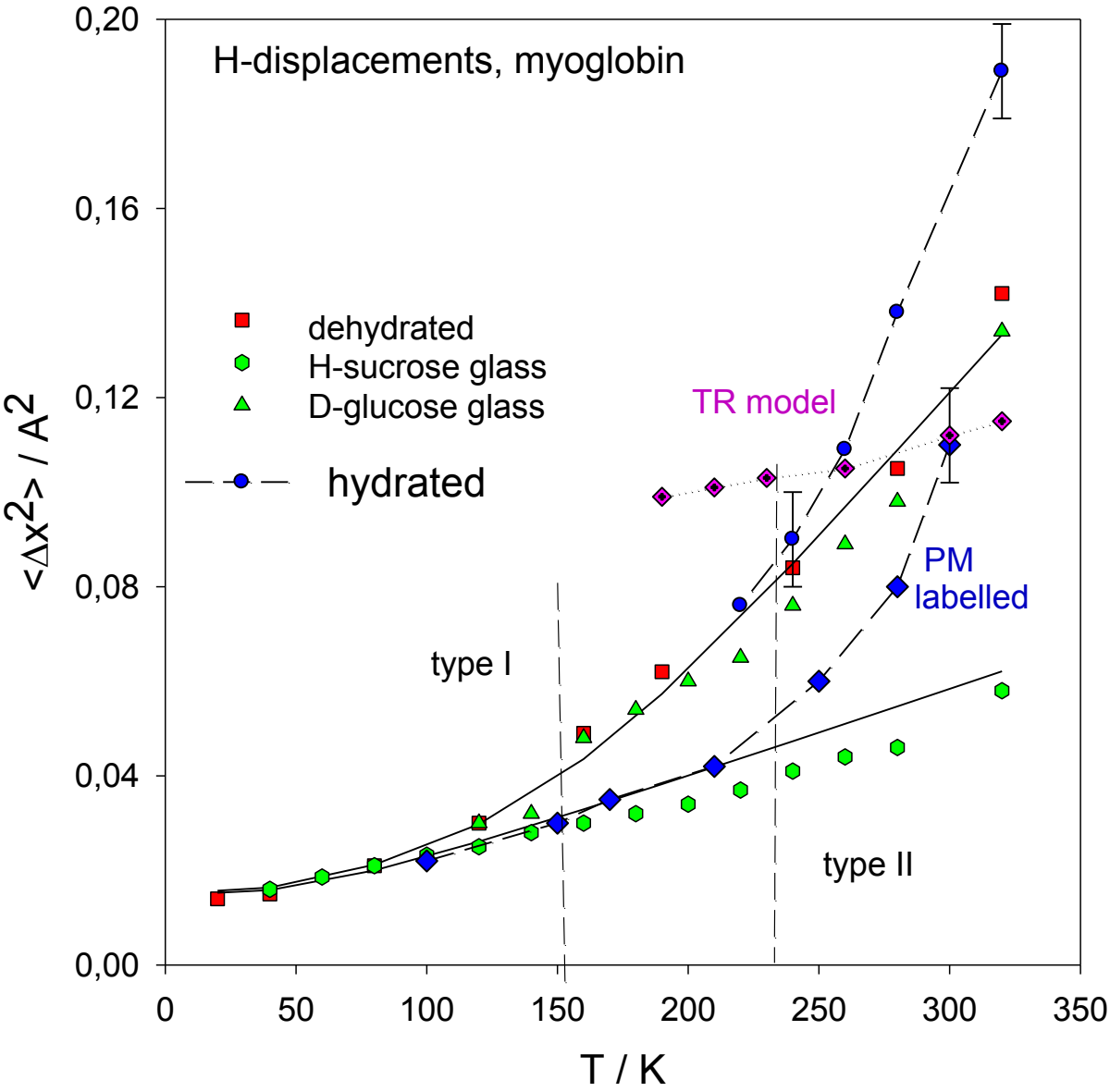
H-displacements, myoglobin
dehydrated
H-sucrose glass
D-glucose glass
hydrated
TR model
PM
labelled
type I
type II
<Δx2> / A2
T / K
0,00
0,04
0,08
0,12
0,16
0,20
0
50
100
150
200
250
300
350

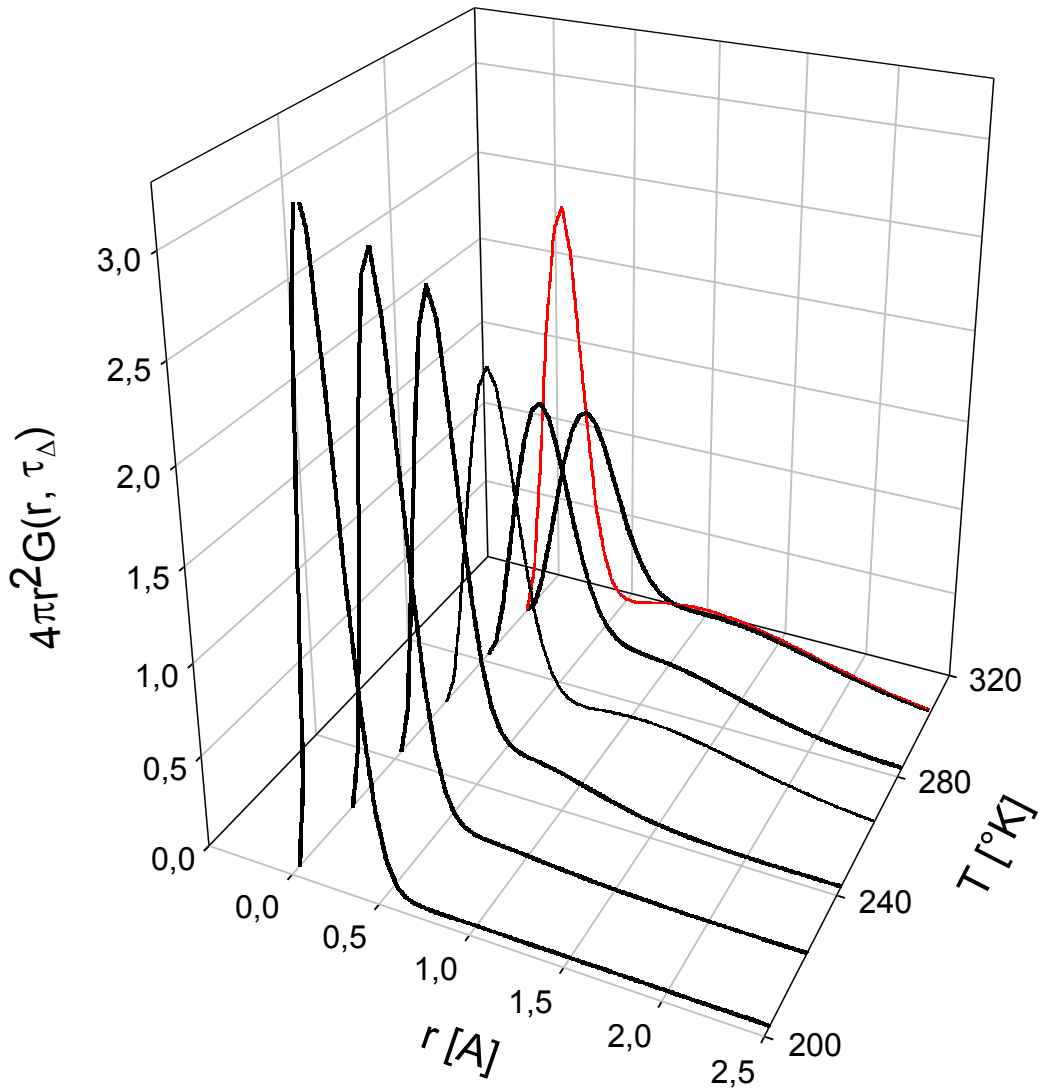
3,0
2,5
2,0
1,5
1,0
0,5
0,0
4πr2G(r, τΔ)
0,0
0,5
1,0
1,5
2,0
2,5
r [A]
320
280
240
200
T [°K]

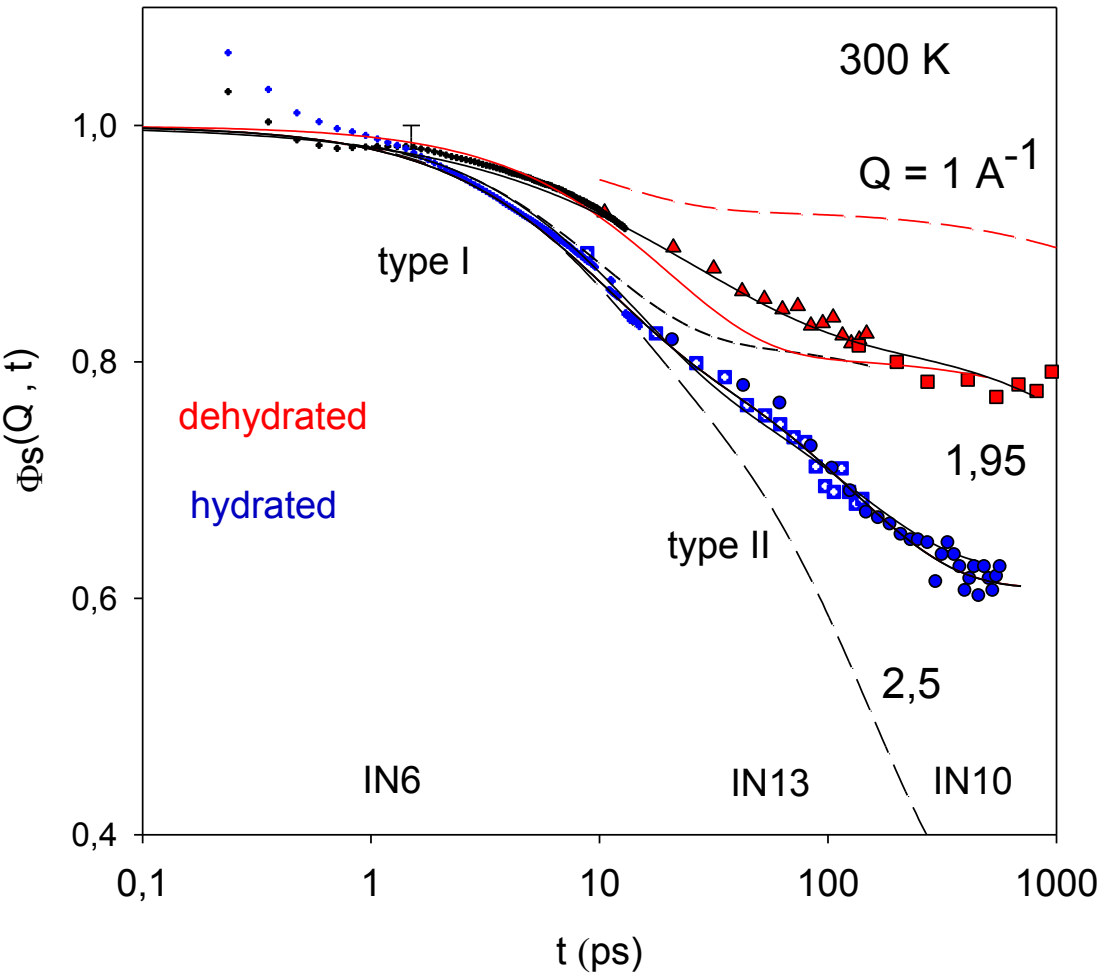
300 K
Q = 1 A-1
type I
dehydrated
hydrated
type II
1,95
2,5
IN6
IN13
IN10
1,0
0,8
0,6
0,4
0,1
1
10
100
1000
Φs(Q , t)
t (ps)

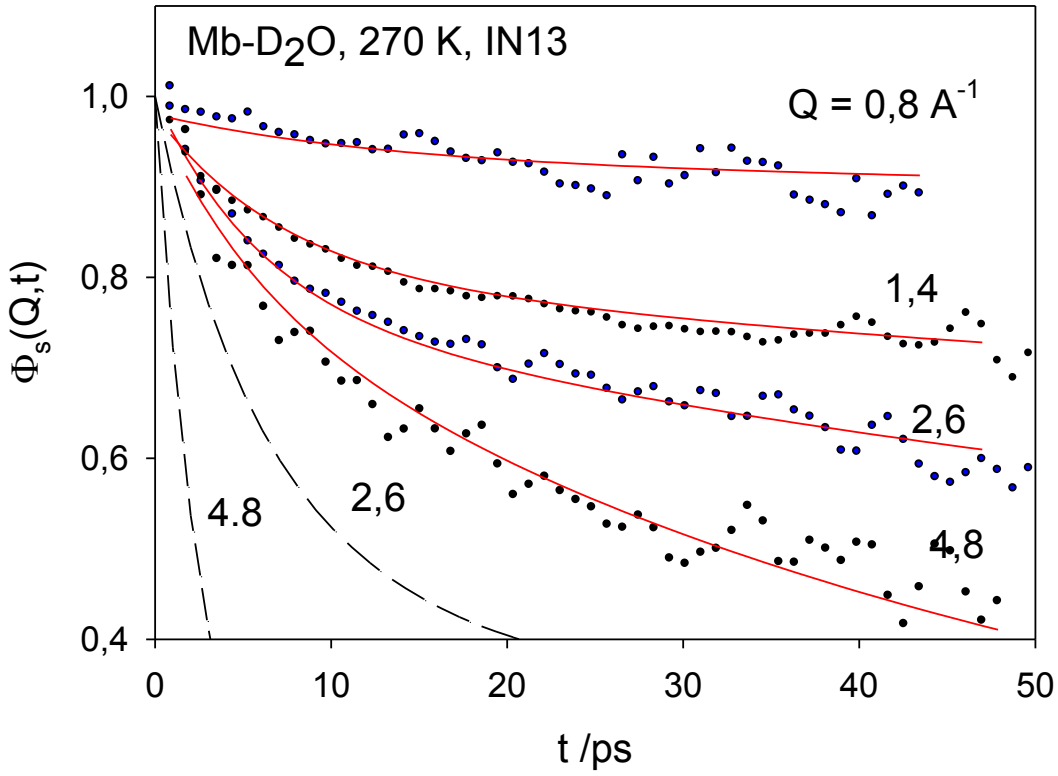
Mb-D2O, 270 K, IN13
Q = 0,8 A-1
1,4
2,6
4,8
2,6
4.8
Φs(Q,t)
t /ps
1,0
0,8
0,6
0,4
0
10
20
30
40
50

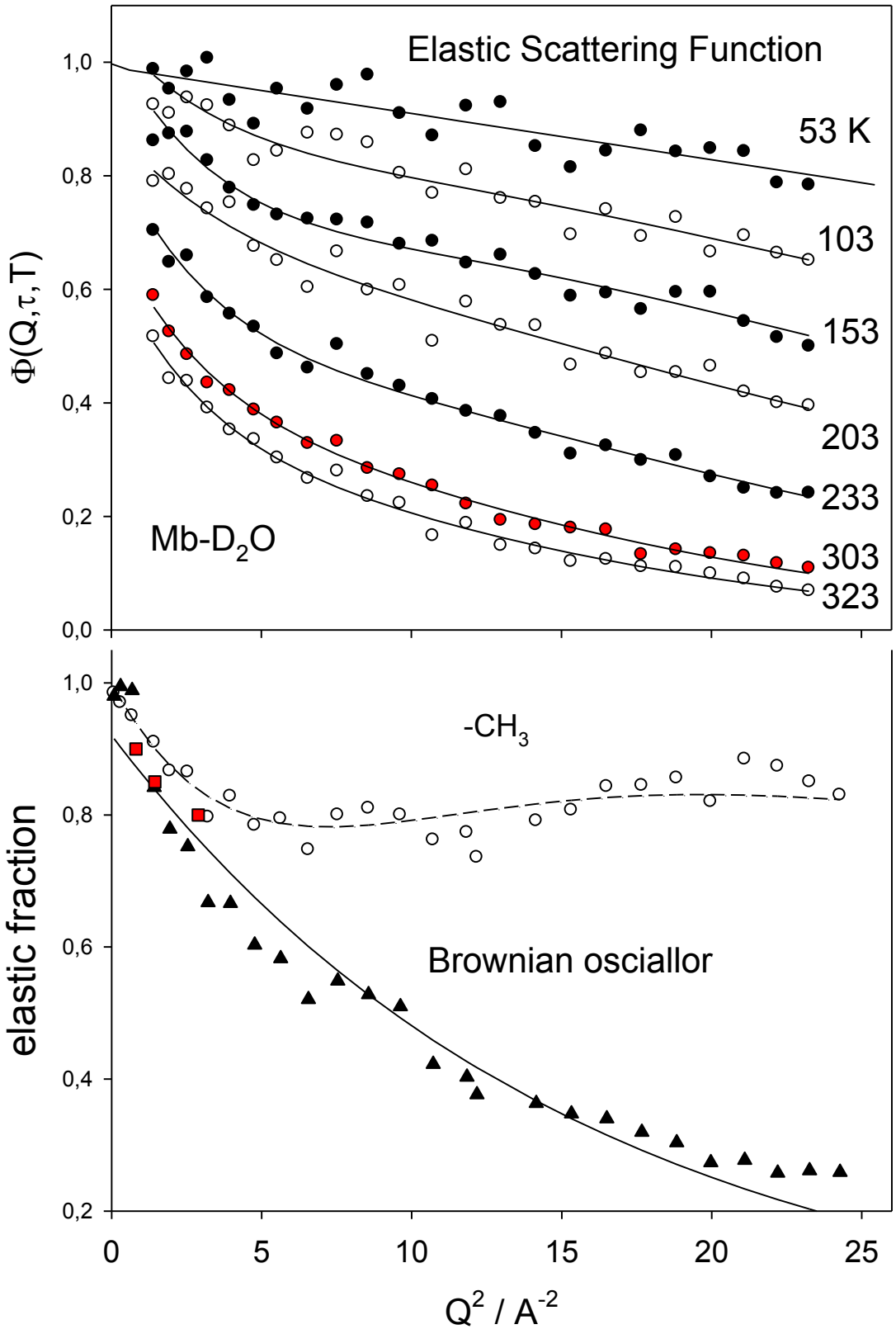
Elastic Scattering Function
53 K
103
153
203
233
303
323
Mb-D2O
Φ(Q,τ,T)
1,0
0,8
0,6
0,4
0,2
0,0
-CH3
Brownian osciallor
elastic fraction
0
5
10
15
20
25
Q2 / A-2

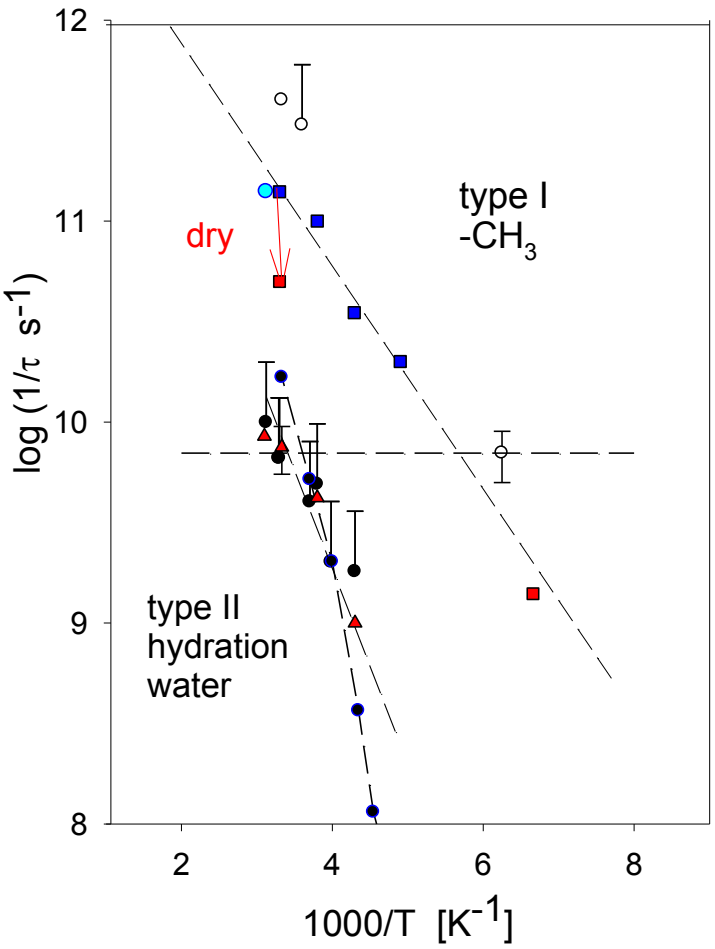
12
11
10
9
8
log (1/τ s-1)
dry
type I
-CH3
type II
hydration
water
2
4
6
8
1000/T [K-1]

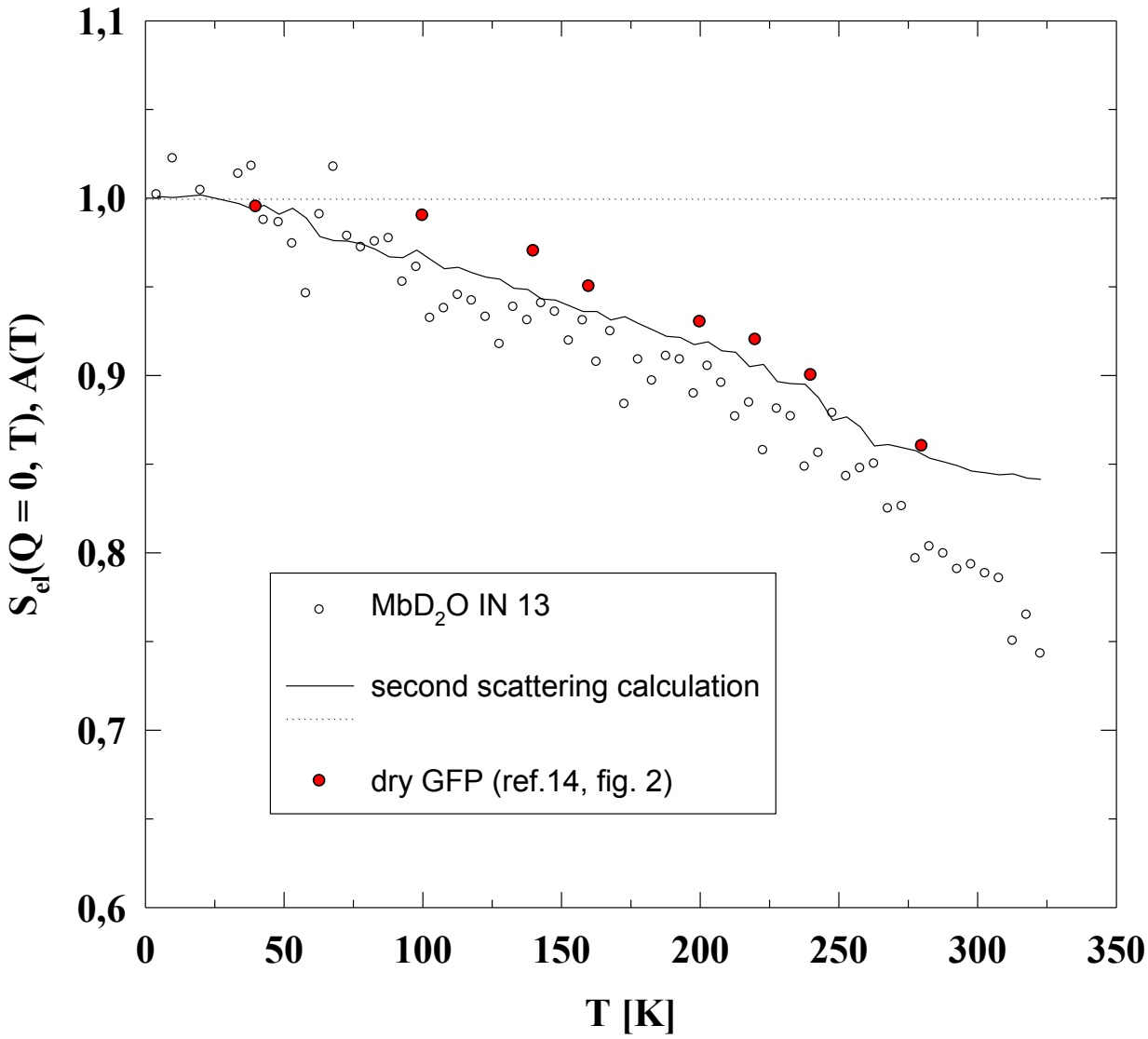
1,1
1,0
0,9
0,8
0,7
0,6
0
50
100
150
200
250
300
350
T [K]
S_el(Q = 0, T), A(T)
MbD2O IN 13
second scattering calculation
dry GFP (ref.14, fig. 2)

Fig. S1: Geometry of the sample cell and definition of the coordinate system used to perform the calculations. Only two scattering events are shown, the relevant parameters are given in the text.

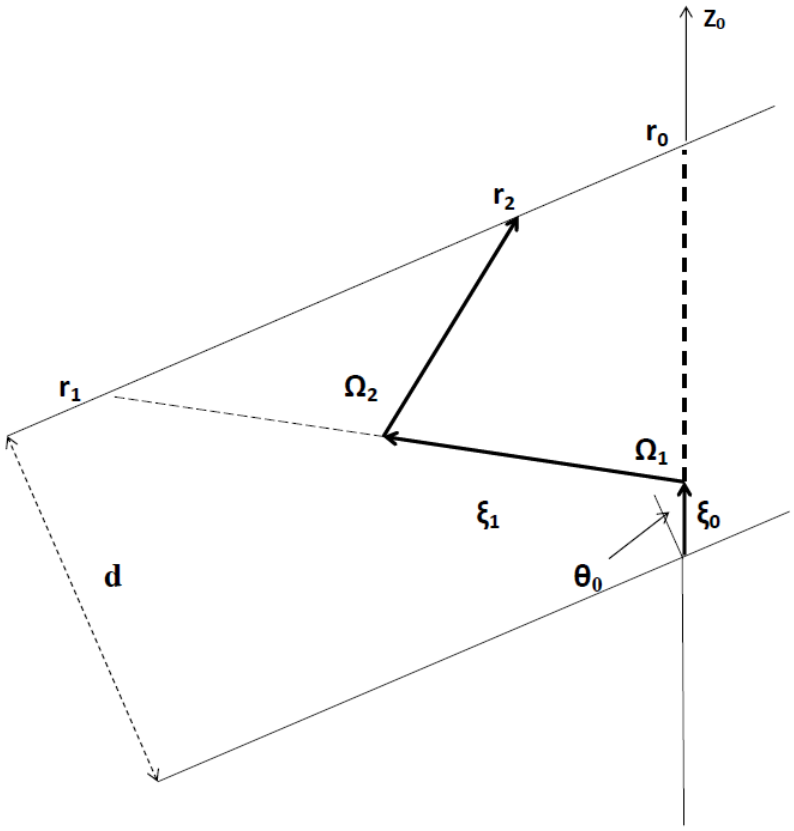

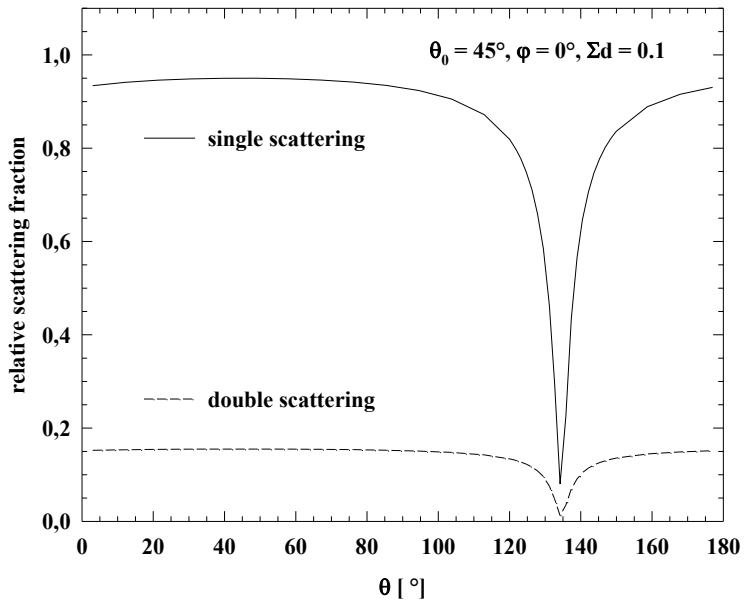

Fig. S2: Transmission factors of the single and double scattered neutrons versus scattering angle for a slap cell which is oriented at 45° relative to the incident beam.

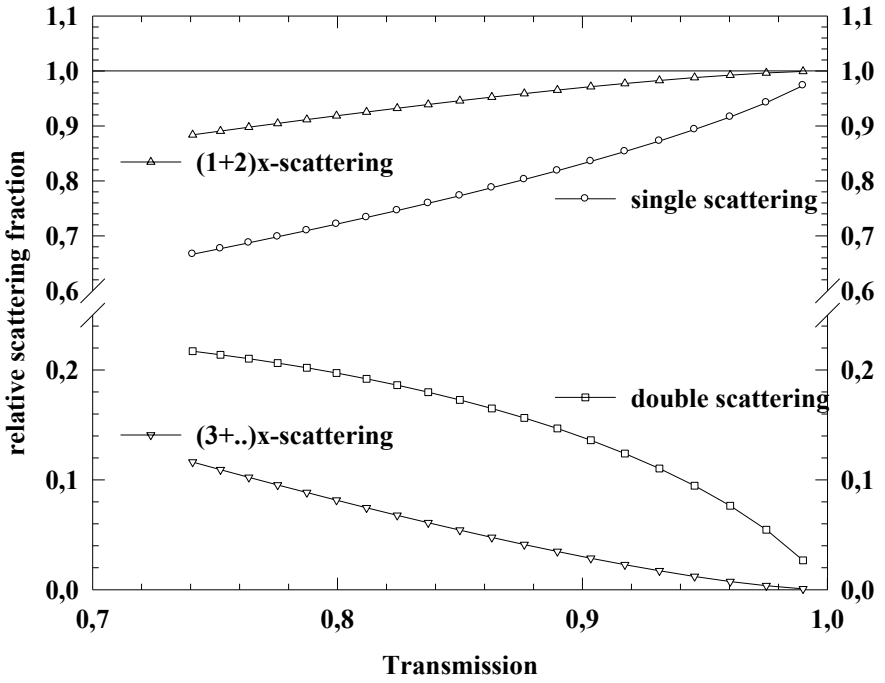

Fig. S3: Single, double and triple scattering fraction versus total transmission T of an elastic and isotropic scattering sample.